Preprints (www.preprints.org) | NOT PEER-REVIEWED | Posted: 18 August 2021 doi:10.20944/preprints202108.0377.v1

Article

Magnetic field perturbations to a soft X-ray activated Fe (II) molecular spin state transition

Guanhua Hao,[1,2] Alpha T. N'Diaye,[2]* Thilini K. Ekanayaka,[1] Ashley S. Dale,[1] Xuanyuan Jiang,[1] Esha Mishra,[1] Corbyn Mellinger,[1] Saeed Yazdani,[3] John Freeland,[4] Jian Zhang,[5] Ruihua Cheng,[3]* Xiaoshan Xu,[1] Peter A. Dowben[1]*

[1] Department of Physics and Astronomy, University of Nebraska-Lincoln, Lincoln, NE 68588-0299, U.S.A; guanhuahao@huskers.unl.edu, thiliniek@huskers.unl.edu, neojxy@gmail.com, emishra@huskers.unl.edu, corbyn.mellinger@huskers.unl.edu, xiaoshan.xu@unl.edu, pdowben1@unl.edu

[2] Advanced Light Source, Lawrence Berkeley National Laboratory, Berkeley, CA 94720, U.S.A.; ghao@lbl.gov, atndiaye@lbl.gov

[3] Physics Department, Indiana University Purdue University-Indianapolis, Indianapolis, IN 46202, U.S.A.; aleas@iupui.edu, syazdani@iupui.edu, rucheng@iupui.edu

[4] Argonne National Laboratory, Advanced Photon Source, Bldg. 431/E003, 9700 South Cass Ave., Argonne IL 60439, U.S.A.; freeland@anl.gov

[5] Molecular Foundry, Lawrence Berkeley National Laboratory, Berkeley, CA 94720, U.S.A.; JianZhang@lbl.gov

* Correspondence: pdowben1@unl.edu; Tel.: +1-402-472-9838 (PAD); atndiaye@lbl.gov; Tel.: +1-510-486-5926 (ATN); rucheng@iupui.edu; Tel.: +1-317-274-6902 (RC)

Abstract: The X-ray induced spin crossover transition of an Fe(II) molecular thin film in the presence and absence of a magnetic field has been investigated. The thermal activation energy barrier in the soft X-ray activation of the spin crossover transition for $[Fe\{H_2B(pz)_2\}_2(bipy)]$ molecular thin films is reduced in the presence of an applied magnetic field, as measured through X-ray absorption spectroscopy at various temperatures. The influence of a 1.8 T magnetic field is sufficient to cause deviations from the expected exponential spin state transition behavior that is measured in the field free case. We find that orbital moment diminishes with increasing temperature, relative to the spin moment in the vicinity of room temperature.

Keywords: Spin crossover, Fe(II), activation barriers, X-ray excitation, , magnetic field effects, $[Fe\{H_2B(pz)_2\}_2(bipy)]$, molecular multiferroic.

1. Introduction

Switching of the spin state, and the accompanying conductivity, with an electric field is a long sought goal with great potential for energy efficient electronics and datastorage. Such magneto-electric coupling has a long history [1], dating back to 1894 [2]. Currently, magneto-electric coupling is being explored in oxides, and raises increasing interest as magneto-electric and multiferroic materials are seen as a pathway to voltage controlled nonvolatile logic [3,4] and memory [4]. There are few investigations of magneto-electric coupling in molecular systems, with clear demonstrations now provided for $[Mn^{3+}(taa)]$ (H_3taa = tris(1-(2-azolyl)-2-azabuten-4-yl)amine) [5,6], and $[Mn^{3+}(3,5\text{-diBr-sal})_2323)]BPh_4$ [7] which undergo a spin state transition and accompanied, more recently, by complementary theory [7,8]. Magneto-electric coupling has also been observed in single crystals of $NiCl_2$–$4SC(NH_2)_2$ [9]. Magnetic fields have been seen to perturb the spin state transition in $[Mn^{3+}(taa)]$ [10], $Fe(1,10\text{-phenanthroline})_2(NCS)_2$ [9], $Fe(phen)_2(NCS)_2$ [11], $[Fe\{H_2B(pz)_2\}_2(bipy)]$ ($H_2B(pz)_2$ = bis(hydrido)bis(1*H*-pyrazol-1-yl)borate, bipy = 2,2′-bipyridine) [12]. Since these latter spin crossover systems all have a static electric dipole that is intrinsically dependent on the spin state, the perturbation of the spin state, say with a

© 2021 by the author(s). Distributed under a Creative Commons CC BY license.

Preprints (www.preprints.org) | NOT PEER-REVIEWED | Posted: 18 August 2021 doi:10.20944/preprints202108.0377.v1

magnetic field, is an example of magneto-electric coupling because there is an accompanying change i the electric polartization.

The fact that the application of a magnetic field tends to relax [Fe{$H_2B(pz)_2$}$_2$(bipy)] back to the low spin state after the soft X-ray excitation to the high spin state [12] suggests that an applied magnetic field may lower the activation barriers separating high spin and low spin states. A lowering of the free energy of the high spin state and a decrease in the activation barrier separating the high spin state from the low spin state, by application of a magnetic field, has also been suggested for $Fe(phen)_2(NCS)_2$ [11]. This magnetic field induced perturbation of the low spin to high spin state barrier is explored here for [Fe{$H_2B(pz)_2$}$_2$(bipy)]. The influence of magnetic fields on the excitation and de-excitation in molecules has been observed before [13–18] and is not unique to spin crossover complexes. These latter studies are not of molecular systems but organics like anthracene and rubrene where this phenomenon arises due to the coupling of a molecule in the electronic singlet ground state with an adjacent molecule in the first excited singlet state to form a correlated triplet-pair state. In the case of [Fe{$H_2B(pz)_2$}$_2$(bipy)], the excitation is accompanied by a spin state change [12,19], and perturbations to the spin state transition, by a magnetic field, is a step toward elucidating the origin of any magneto-electric coupling.

2. Results

2.1. Magnetic Field Effects On The Excitation Spin Crossover

As previously reported [12], a soft X-ray irradiation excites [Fe{$H_2B(pz)_2$}$_2$(bipy)] thin films on $NiCo_2O_4$(111) from the low spin state to the high spin state. Furthermore, an alternating magnetic field has been shown to perturb the [Fe{$H_2B(pz)_2$}$_2$(bipy)] thin film spin state on $NiCo_2O_4$(111) [12]. Here we demonstrate how a static applied magnetic field subtly changes the characteristics of the spin state evolution induced by incident X-rays.

The spin state occupancy of [Fe{$H_2B(pz)_2$}$_2$(bipy)] Fe(II) thin films may be ascertained from the X-ray absorption spectra (XAS) [12,19-27]. In the low spin (LS) state of the [Fe{$H_2B(pz)_2$}$_2$(bipy)] molecule, the *3d* electrons occupy the t_{2g} orbitals in pairs leaving the e_g orbitals empty. The empty e_g orbitals are generally observed in the Fe L_3 edge ($2p_{3/2}$) X-ray absorption spectra as a major feature at a photon energy around 708.9 eV. In the high spin (HS) state configuration, the e_g orbitals are partially populated while the t_{2g} orbitals become partly depopulated, and thus contribute features in the XAS spectra at lower photon energies leading to a decrease of the peak intensity at 708.9 eV and an increase of the t_{2g} shoulder around 706.8 eV. as shown in Figure 1. The asymmetry between the empty t_{2g} and empty e_g state peaks signatures is a measure of the fraction of molecules in the high spin state as has been shown experimentally [12,19-27]. Such analysis of the XAS spectra has also been shown to be in agreement with theory as the spin state occupancy changes [20].

There is an evolution of the XAS spectra of [Fe{$H_2B(pz)_2$}$_2$(bipy)] thin films, on $NiCo_2O_4$(111), that occurs with an incident X-ray fluence, as seen in Figure 1. From these spectra, there is clear evidence of an evolution of the average spin state, from a low spin state, towards larger fractions of high spin state with increasing incident X-ray fluence, , as reported elsewhere [12]. This soft X-ray excitation into the high spin state has been demonstrated to be reversable [12].

This evolution of the average spin state occupancy is perturbed by the presence of an external magnetic field. The XAS spectra indicate differences in the spin state occupancy for identical X-ray exposures where the only variable is the applied external magnetic field. Figure 1a shows spectra from the time evolution at 300 K, measured without any magnetic field, as well as measured with an applied field of 1.8 T. While the e_g to t_{2g} peak ratios for the initial state are identical, the XAS spectra, with and without an applied magnetic field, differ markedly after 3000 s of the X-ray exposure. Analysis of the relative intensity of the e_g and t_{2g} XAS features show that in the absence of an applied magnetic field, the [Fe{$H_2B(pz)_2$}$_2$(bipy)] molecular thin film resides well more than 80% in the high spin state. In the presence of a 1.8 T out-of-plane applied magnetic field, however, the

Preprints (www.preprints.org) | NOT PEER-REVIEWED | Posted: 18 August 2021 doi:10.20944/preprints202108.0377.v1

[Fe{$H_2B(pz)_2$}$_2$(bipy)] molecular thin film, on $NiCo_2O_4$(111), resides in a mixed spin state with a relatively smaller high spin state fraction (i.e. <70% high spin), as indicated from the XAS spectra. Differences in the spin state occupancy are evident at other temperatures as well (Figure 1b and Supplementary Material). This is consistent with prior observations that the magnetic field has been seen to perturb the [Fe{$H_2B(pz)_2$}$_2$(bipy)] thin film spin state on $NiCo_2O_4$(111) [12].

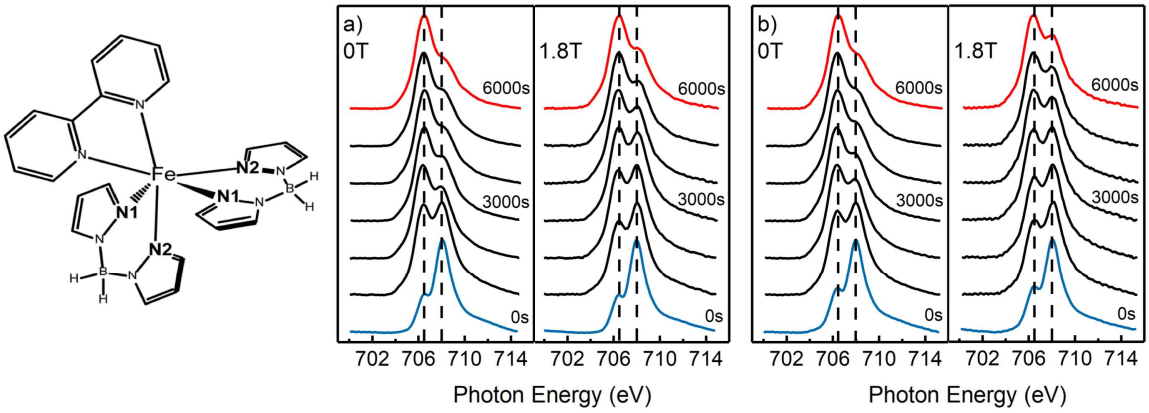

Figure 1. The time evolution of the X-ray absorption spectra of [Fe{$H_2B(pz)_2$}$_2$(bipy)] thin films, on $NiCo_2O_4$(111), with and without an applied 1.8 T magnetic field, under a constant incident X-ray fluence at a) 300 K and b) 200 K. The spectra in blue are indicative of a film in largely low spin state (roughly 30% high spin), while the spectra in red are largely indicative of high spin state. At the left is a schematic of [Fe{$H_2B(pz)_2$}$_2$(bipy)] ($H_2B(pz)_2$ = bis(hydrido)bis(1H-pyrazol-1-yl)borate, bipy = 2,2′-bipyridine). Hydrogens are omitted for clarity.

To clarify this soft X-ray induced spin state evolution of [Fe{$H_2B(pz)_2$}$_2$(bipy)] molecular thin film on $NiCo_2O_4$(111), with and without an applied magnetic field, we extracted the occupancy evolution from series of spectra taken over the course of 6000 s (the data for 200 K and 300 K are plotted in Figure 2). All temperatures shown here are above the spin crossover temperature of the pure molecule which is generally observed to occur at about 160 K [20–22,26,28-30]. Yet without an incident X-ray fluence, the [Fe{$H_2B(pz)_2$}$_2$(bipy)] molecular thin films on $NiCo_2O_4$(111) are locked in the low spin state by the interface to the substrate [12]. The evolution towards the high spin state is the result of the X-ray fluence overcoming the tendency of the substrate to lock the [Fe{$H_2B(pz)_2$}$_2$(bipy)] molecular thin film in the low spin state. In the presence of an applied magnetic field, the initial increase towards the high spin state occupancy is rapid (red shaded curves in Figure 2). We denote this initial increase in high spin state occupancy as regime I. This is followed by a slower and more linear increase in high spin state occupancy (the blue shaded curves in Figure 2). We denote this latter evolution toward the high spin state, in an applied magnetic field, as regime II. This evolution towards high spin state occupancy behavior, in an applied magnetic field, differs significantly from the exponential increase in high spin state occupancy observed in the absence of an applied magnetic field (black shaded curves in Figure 2).

Preprints (www.preprints.org) | NOT PEER-REVIEWED | Posted: 18 August 2021 doi:10.20944/preprints202108.0377.v1

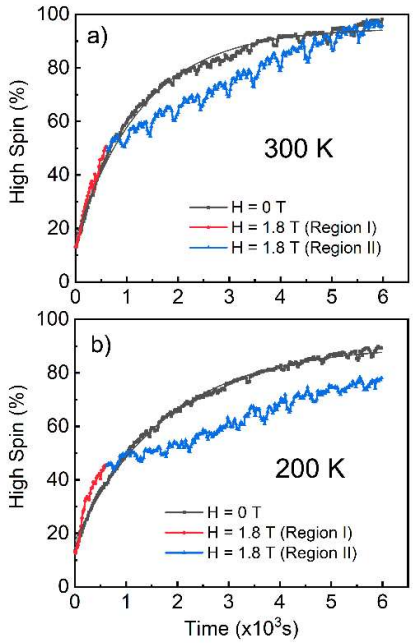

Figure 2. The evolution of the high spin state occupancy in the [Fe{$H_2B(pz)_2$}$_2$(bipy)] thin films, on $NiCo_2O_4$(111), that accompany an incident soft X-ray fluence are plotted for a) 300 K and b) 200 K, in the absence of an applied magnetic field (black) as well as in the presence of a 1.8 T applied magnetic field (red and blue). Exponential fits to the high spin state conversion in the absence of an applied magnetic field are indicated.

The excitation to the high spin state, in the presence of the X-ray fluence and an applied magnetic field , is complcated by competing process, which are also evident as there are fluctuations in the evolution to the high spin state (Figure 2, blue regions). These fluctuations, on the time scale of tens to 200 seconds in regime II (Figure 2), are both magnetic field and temperature dependent, thus unlikely to be instrumental, but are indicative of competing dynamic processes whose nature should be investigated but is outside ths cope of this work. Here we focus on the effects on a long timescale of tens of minutes to hours.

2.2. The Temperature Dependence of The Spin To Orbital Moment Ratio

A thermal component to the magnetic moment and the spin state transition must occur through the ligand field. This implies the orbital moment is more susceptible to temperature than the spin moment in the high spin state. To test this, we measured the high spin state spin to orbital moment of [Fe{$H_2B(pz)_2$}$_2$(bipy)] thin films in the high spin state on a substrate where the influence of the substrate on the spin state of the [Fe{$H_2B(pz)_2$}$_2$(bipy)] thin film is known to be minimal, i.e. graphite [25,26]. Temperatures in the vicinity of 300 K are well above the spin state transition of about 160 K [20–22,26,28-30] as noted above, but thermal effects are seen in the orbital contribution to the local moments, as seen in X-ray circular dichroism (XMCD) spectra at the Fe 2p core thresholds of [Fe{$H_2B(pz)_2$}$_2$(bipy)] thin films on graphite, as seen in Figure 3.

The normalized XMCD data, for the Fe $2p_{3/2}$ and $2p_{1/2}$ (L3 and L2 edges), for [Fe{$H_2B(pz)_2$}$_2$(bipy)] thin films on graphite, is shown in Fig. 3a for different temperatures. After subtracting a linear background, sum rules were applied to calculate the average spin moment based on the relative integrated XMCD signals, as shown in Figure 3b, following the procedure of Chen et al. [31]. The moments obtained from XMCD will be only a small fraction of the actual Fe(II) moments, largely because the [Fe{$H_2B(pz)_2$}$_2$(bipy)] moments are not saturated [32], but also because the thin films contain both chiral isomers each of which respond differently to circularly polarized light, the light is elliptical not

Preprints (www.preprints.org) | NOT PEER-REVIEWED | Posted: 18 August 2021 doi:10.20944/preprints202108.0377.v1

perfectly circularly polarized, there is likely a misalignment of light angular momentum vector with respect to the magnetic moment and there are Fresnel boundary conditions in play. Yet in the high spin state a local moment is likely the case. As seen in Figure 4a, the relative spin moment S_z (red), extracted from the XMCD spectra, is relatively insensitive to small changes in temperature while the relative orbital moment L_z (blue) decreases significantly with a small increase in temperature for the [Fe{$H_2B(pz)_2$}$_2$(bipy)] on graphite sample.

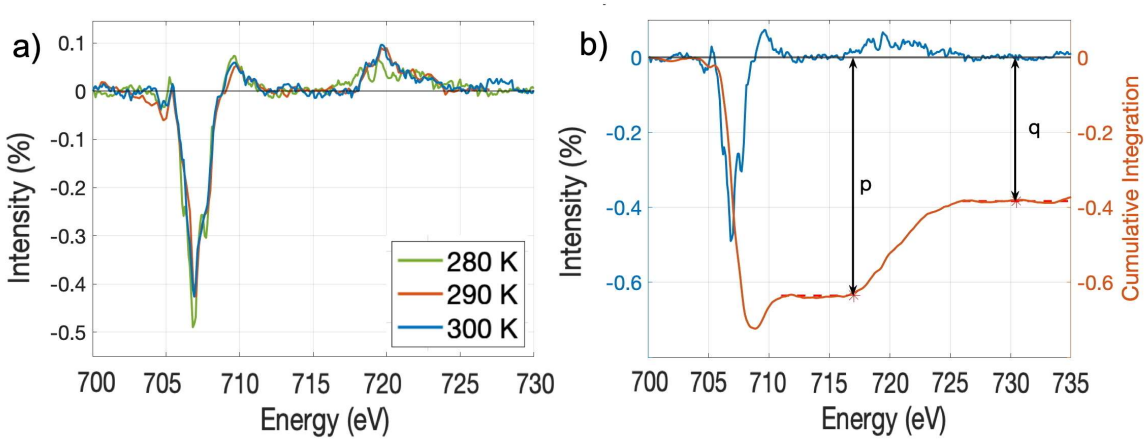

Figure 3. The Fe $2p_{3/2}$ and $2p_{1/2}$ (L3 and L2 edges) XMCD spectra of 30 nm [Fe{$H_2B(pz)_2$}$_2$(bipy)] thin films on graphite. (a) The spectra were taken at 280 K (green), 290 K (red) and 300 K (blue). (b) The Fe $2p_{3/2}$ and $2p_{1/2}$ (L3 and L2) XMCD spectrum taken at 280 K (blue curve) compared to the integrated XMCD signal (red curve). The XMCD spectra are plotted as a percent of the total X-ray absorption spectra.

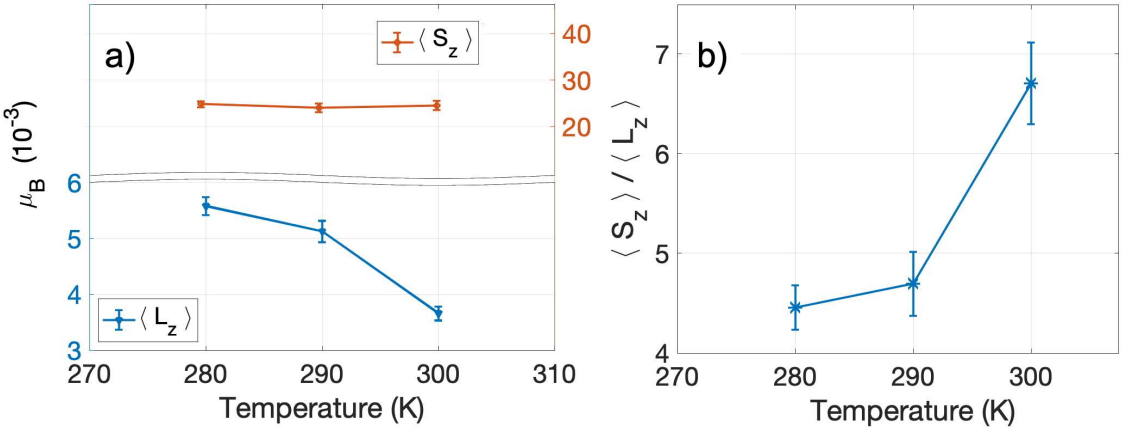

Figure 4. The temperature dependence of the relative spin S_z and orbital L_z moments extracted from Fe(II) XMCD taken from a 30 nm [Fe{$H_2B(pz)_2$}$_2$(bipy)] thin film on graphite. (a) The temperature dependent spin moment (red plot) and orbital moment (blue plot) of Fe (II). (b) The ratio of spin moment S_z to orbital moment L_z as a function of temperature in the vicinity of room temperature.

The expected spin to orbital moment ratio should lie between 3 and 6, for an Fe(II) spin crossover complex, like [Fe{$H_2B(pz)_2$}$_2$(bipy)], in the high spin state [33]. Estimating the ratio of the spin to orbital moment from the XMCD spectra as $\langle S_z \rangle / \langle L_z \rangle = (9p - 6q)/2q$ [31], with p and q determined from the integrated XMCD plots, as indicated in Figure 3, we find that the $\langle S_z \rangle / \langle L_z \rangle$ from about 4.5 to nearly 7 (Figure 4b). This is reasonably consistent with expectations. More surprising is that the spin to orbital moment ratio

Preprints (www.preprints.org) | NOT PEER-REVIEWED | Posted: 18 August 2021 doi:10.20944/preprints202108.0377.v1

$\langle S_z \rangle / \langle L_z \rangle$ varies widely with small changes in temperature (Figure 4b) as a result of the changes in orbital moment with temperature (Figure 4a). This indicates that the orbital moment of $[Fe\{H_2B(pz)_2\}_2(bipy)]$ is very soft with respect to temperature changes.

3. Discussion

It is clear that a static applied magnetic field has an influence on the X-ray induced transition from the low spin to high spin state for $[Fe\{H_2B(pz)_2\}_2(bipy)]$ molecular thin films on $NiCo_2O_4(111)$. We note that, in the absence of an applied magnetic field, the observed exponential increase in high spin state occupancy for $[Fe\{H_2B(pz)_2\}_2(bipy)]$ molecular thin films on $NiCo_2O_4(111)$, between 200 K and 300 K (black shaded curves in Figure 2), resembles the exponential increase in high spin state occupancy observed as a result of X-ray beam induce low spin state (LS) to high spin state (HS) transitions at low temperatures (5 K), seen for $[Fe\{H_2B(pz)_2\}_2(bipy)]$ molecular thin films on graphite [25,26]. This soft X-ray-induced excited spin state trapping (SOXIESST), seen for $[Fe\{H_2B(pz)_2\}_2(bipy)]$ molecular thin films on graphite at below 40 to 50 K, occurs because the graphite substrate does not lock the spin state of the $[Fe\{H_2B(pz)_2\}_2(bipy)]$ molecular thin films into the low spin state [25,26], while in contrast to the case graphite of the weakly interacting graphite subsrate, a spin state locking effect occurs for $[Fe\{H_2B(pz)_2\}_2(bipy)]$ molecular thin films on $NiCo_2O_4(111)$ [12].

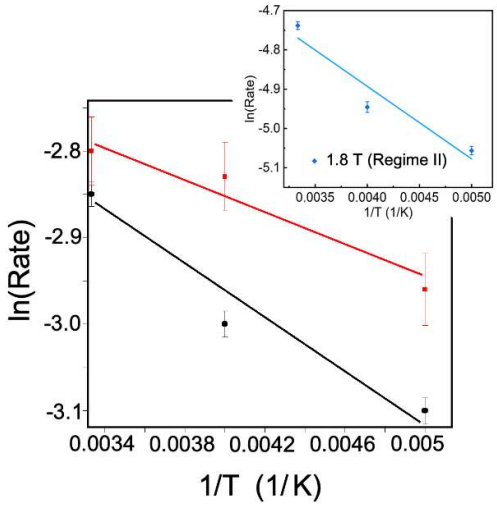

Figure 5. The temperature dependent Arrhenius plots of the conversion rate to a high spin state for $[Fe\{H_2B(pz)_2\}_2(bipy)]$ thin films on $NiCo_2O_4(111)$, induced by a soft X-ray fluence. In the absence of an applied magnetic field this temperature dependence indicates a thermal component of the activation energy of 14.5±1.5 meV (black). The Arrhenius plot for the initial period when 1.8 T external magnetic field is applied (regime I, Figure 2) suggests a thermal component of the activation energy of 7.2±2 meV (red). The inset is the Arrhenius plot for the following 1.8 T transition to the high spin state when a significant fraction of the $[Fe\{H_2B(pz)_2\}_2(bipy)]$ thin film on $NiCo_2O_4(111)$ has converted to the high spin state (regime II, Figure 2) and indicates a thermal component of the activation energy of 15.9±2.7 meV (blue).

The temperature dependence of the spin state evolution provides an opportunity to estimate the thermal component of the activation barrier in this X-ray induced transition. Arrhenius rate plots with temperature (Figure 5) were calculated based on the high spin occupancy results shown above, based on the initial rates of spin state. In the absence of an applied magnetic field, an activation barrier of 14.5±1.5 meV per molecule is calculated. The initial rates of $[Fe\{H_2B(pz)_2\}_2(bipy)]$ conversion to high spin state in an applied magnetic field (regime I, in Figure 2) suggests a somewhat lower activation energy of 7.2±2 meV. After a significant fraction of the film has already converted to the high spin state (regime II in Figure 2), the activation energy in an applied magnetic field is again restored

Preprints (www.preprints.org) | NOT PEER-REVIEWED | Posted: 18 August 2021 doi:10.20944/preprints202108.0377.v1

to 15.9±2.7 meV, as indicated by the inset in Figure 5. A magnetic field dependence on the free energy and activation barrier has been suggested for the $Fe(phen)_2(NCS)_2$ spin state transition [11], so the effect of larger magnetic fields than exploited here is of considerable interest.

The decrease in the thermal component to the activation energy can also explain the conversion rate curves of Figure 2 for this X-ray induced transition. When the $[Fe\{H_2B(pz)_2\}_2(bipy)]$ high spin state occupancy increases enough, it is clear that X-ray induced photo-excitation to the high spin state of the small amount of material remaining in the low spin state begins to compete with the conversion of the large amount of film in the high spin state back to the low spin state favored by the $[Fe\{H_2B(pz)_2\}_2(bipy)]$ interaction with the $NiCo_2O_4(111)$ substrate. This is certainly consistent with a nearly 50% decline in activation energy with the application of a magnetic field. Due to possible inhomogeneities, such as a distribution of crystalline grain sizes, the thermal energy barriers towards conversion to the high spin state or back conversion to the low spin state could be only lowered for part of the film, while either unchanged or retaining a different value for another part of the film.

The presence of this low spin state back-conversion prevents a full excitation into the high spin state when there is an applied magnetic field. Indeed, this enhanced back-conversion to the low spin state has been seen previously for $[Fe\{H_2B(pz)_2\}_2(bipy)]$ thin films, as a result of applied alternating magnetic field [12]. It is then the competition between excitation to the high spin state and the enhanced back conversion to the low spin state that then leads to the apparent increase in the thermal component of the activation energy. The appearance of two regimes in the soft X-ray fluence induced evolution (regime I and II in Figure 2) can be explained by expanding the model to include two separate conversion rates, as indicated in models of the spin crossover plotted in Figure 6. This difference in $[Fe\{H_2B(pz)_2\}_2(bipy)]$ spin state conversion rates could either be induced by heterogeneity or by a different behavior of the film depending on the proximity to the substrate or vacuum interface, as it has been observed before [21].

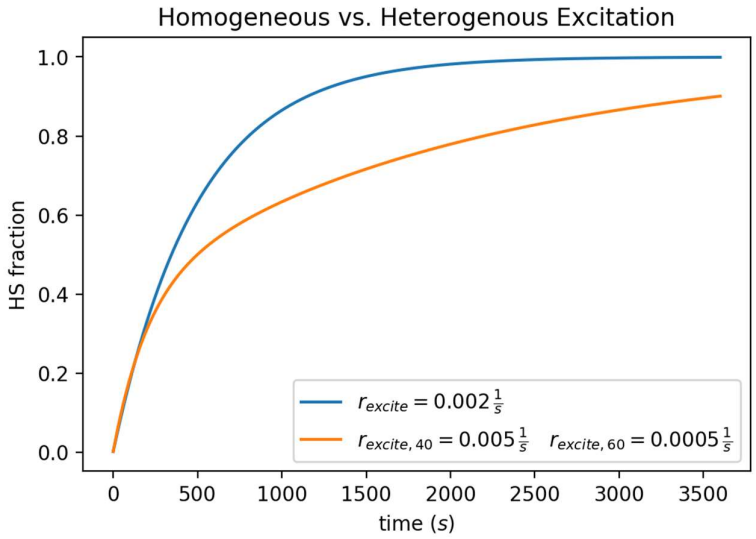

Figure 6. A simulation of the evolution of the high spin state occupancy in the $[Fe\{H_2B(pz)_2\}_2(bipy)]$ molecular thin film assuming a simple excitation rate uniformly throughout the film (blue) and an inhomogeneous excitation process where 40 % of the film is activated with one constant rate and 60% of the film at a lower rate that is 10% of the higher rate (orange).

A single molecule could gain $E = H \cdot \Delta m$ energy for a moment change under the presence of a magnetic field, but with a moment change of $\Delta m=4\ \mu_B$ and an applied field

Preprints (www.preprints.org) | NOT PEER-REVIEWED | Posted: 18 August 2021 doi:10.20944/preprints202108.0377.v1

H=1.8 T, this gain would be 0.42 meV at most. In fact, because of finite temperature effects, leading to moment canting, the actual energy in the vicinity of room temperature would be much smaller. A magnetic field dependent change on an energy scale of several meV is well above that level and can only be explained by cooperative coupling of several molecules. This suggests that the spin crossover occurs collectively with a cluster of molecules, consistent with previous work [21,23] which indicates spin-state domains in $Fe\{H_2B(pz)_2\}_2(bipy)$] thin films.

These activation energy values of 14.5 to 15.9 meV per molecule are close to the 14 to 18 meV value of the thermal activation energy component of the X-ray fluence induced transition to the high spin state for $[Fe\{H_2B(pz)_2\}_2(bipy)]$ locked in the low spin state with zwitterion additions [27]. This similarity suggests that the energetics involved in locking of $[Fe\{H_2B(pz)_2\}_2(bipy)]$ in the low spin state by zwitterion additions or by a $NiCo_2O_4(111)$ substrate are comparable.

The presence of thermal activation barriers does imply that the ligand field of $[Fe\{H_2B(pz)_2\}_2(bipy)]$ is subject to temperature variations. The thermal effects on the ligand field is supported by the significal changes in the relative orbital moment, with temperature as validated by the XMCD measurements. As noted above, spin to orbital moment ratio $\langle S_z\rangle/\langle L_z\rangle$ for $[Fe\{H_2B(pz)_2\}_2(bipy)]$ thin films on graphite varies widely with small changes in temperature (Figure 4b). For such a wide variation of $\langle S_z\rangle/\langle L_z\rangle$ to occur, in response to small temperature changes, the ligand field for $[Fe\{H_2B(pz)_2\}_2(bipy)]$ must be sensitive to temperature. This sensitivity of the ligand field, evident in the wide variation in $\langle L_z\rangle$ with small changes in temperature, also provides some explanation as to why there is a thermal component of the activation energy barrier in the soft X-ray activation of the spin crossover transition for $[Fe\{H_2B(pz)_2\}_2(bipy)]$ molecular thin films.

Magnetic anisotropy is very characteristic of local moment molecular systems [34], yet the effect of an anisotropy barrier resulting from the substrate [19,21] or cooperative effects [21,23] cannot be excluded by any data presented here data. The fact that this ligand field is both temperature sensitive and that there are known cooperative effects [21,23,25,26] indicates that a magnetic anisotropy is a very real possibility.

4. Materials and Methods

The $[Fe\{H_2B(pz)_2\}_2(bipy)]$ molecule was synthesized as described elsewhere [20], and characterized as noted elsewhere [12,19–23,28]. A schematic diagram of $[Fe\{H_2B(pz)_2\}_2(bipy)]$ is shown in Figure 1. The X-ray absorption spectroscopy measurements of $[Fe\{H_2B(pz)_2\}_2(bipy)]$ thin films were performed at the Advanced Light Source at Lawrence Berkeley National Laboratory on the bending magnet beamline 6.3.1 at a reduced storage ring current of 15 mA using circularly polarized, negative helicity photons. Spectra were taken both in the absence of an applied magnetic field as well as in the presence of a 1.8 T applied magnetic field, with the field applied perpendicular to the surface of the film. The incident photon flux was in the region of 10^{11} photons s^{-1} 0.1%BW^{-1}. The sample temperature was allowed to equilibrate for 2 hours at each temperature before the measurement ensuring not only a stable temperature but also negligible positional drift with respect to the ~80 μm diameter of the x-ray beam along the cryostat direction (the X-ray beam spot size is 180 μm x 80 at the Advanced Light Source beamline 6.3.1). The total electron yield mode was used to measure the absorption across the Fe $2p_{3/2}$ (L_3) edge, as was done in previous studies [12,19-24] that have also confirmed that the x-ray induced excitation into the high spin is reversible.

As in previous studies [12], $[Fe\{H_2B(pz)_2\}_2(bipy)]$ was thermally evaporated [12,19,21–24,28] on nickel cobaltate ($NiCo_2O_4(111)$) (~100 nm) thin films grown on $Al_2O_3(0001)$ substrates by pulsed laser deposition (PLD) [12]. The substrate temperature for thermal evaporation was at -33 °C, and the growth rate for $[Fe\{H_2B(pz)_2\}_2(bipy)]$ molecules was 0.02 Å/s under the high vacuum (1.0×10^{-7} Torr). The $[Fe\{H_2B(pz)_2\}_2(bipy)]$ SCO molecular films were nominally 15 nm thick, the film thickness was measured by a quartz thickness monitor. After the deposition, the samples were naturally warmed up to room

Preprints (www.preprints.org) | NOT PEER-REVIEWED | Posted: 18 August 2021 doi:10.20944/preprints202108.0377.v1

temperature. It has been established [12] that a $NiCo_2O_4$(111) substrate will lock a 10 to 15 nm [Fe{$H_2B(pz)_2$}$_2$(bipy)] spin crossover molecular thin film largely in the low spin state, almost independent of temperature. The magnetic properties of the $NiCo_2O_4$(111) thin films have been studied systematically [35,36]. In particular, for the semiconducting $NiCo_2O_4$(111) films, grown on Al_2O_3(001) film, ferrimagnetism occurs below T_c=330 K. Although the easy axis is not along the out-of-plane direction, there is significant remanence (>50% saturation value) with a coercivity about 1000 Oe [35]. These experimentally advantageous parameters make $NiCo_2O_4$(111) very suitable as the substrate for the [Fe{$H_2B(pz)_2$}$_2$(bipy)] thin film. Because of the stability of the [Fe{$H_2B(pz)_2$}$_2$(bipy)] thin film on $NiCo_2O_4$(111), the experiments can be repeated at several different temperatures.

To get into the high spin state, a soft X-ray fluence has been seen to be effective, and as noted previously, this is seen for [Fe{$H_2B(pz)_2$}$_2$(bipy)] on $NiCo_2O_4$(111) [12]. The experiments were repeated at different temperatures on a fresh spot of the [Fe{$H_2B(pz)_2$}$_2$(bipy)] thin film on $NiCo_2O_4$(111), to ensure otherwise equivalent starting conditions for each measurement. In addition, control experiments with a swapped order of in-field and field free measurement conditions and various stabilizations time of the electromagnet were made to exclude thermal drift.

Additional X-ray absorption spectroscopy (XAS) and magnetic circular dichroism (XMCD) characterization of [Fe{$H_2B(pz)_2$}$_2$(bipy)] thin films were performed at Advanced Photon Source beamline 4-ID-C at Argonne National Laboratory [37,38]. The spot size is roughly 1 mm at Advanced Photon Source beamline 4-ID-C. For these XMCD measurements, the samples consisted of nominal ~30 nm of [Fe{$H_2B(pz)_2$}$_2$(bipy)] thin films on a HOPG substrates, again prepared using thermal evaporation. Graphite, as a substrate, is better suited for studies of magnetic field perturbations of [Fe{$H_2B(pz)_2$}$_2$(bipy)] in the high spin state than $NiCo_2O_4$(111), as graphite is known as a substrate where [Fe{$H_2B(pz)_2$}$_2$(bipy)] undergoes a complete thermal- and light-induced spin transition even in the monolayer limit [25,26], very much like the powder, so substrate effects on the [Fe{$H_2B(pz)_2$}$_2$(bipy)] thin film are thus minimal. Measurements of the Fe $L_{2,3}$-edge XMCD spectra were taken in total electron yield mode with a 2 T magnetic field applied nearly perpendicular to the sample surface. In order to eliminate some of the artifacts, the final spectrum was obtained from the difference of two spectra taken at $\pm$ 2 T magnetic field. To study the temperature effects, XMCD data was obtained at several temperatures near room temperature, T = {280 K, 290 K, 300 K}.

5. Conclusions

There is now clear evidence that a moderate, static magnetic field can affect the soft X-ray induced conversion of [Fe{$H_2B(pz)_2$}$_2$(bipy)] thin film spin state, locked in the low spin state by a $NiCo_2O_4$(111) substrate. The changes in the activation energy and in the soft X-ray photo-excitation enhanced spin crossover transition indicates an influence of the magnetic field on the thermal component of the spin-crossover transition. In the presence of a large magnetic field (2T) the ligand field is seen to be sensitive to variations in temperature as the relative orbital moment changes dramatically with small changes in temperature. This is consistent with a temperature dependence of the the soft X-ray induced conversion of [Fe{$H_2B(pz)_2$}$_2$(bipy)] thin film spin state. Deepening the understanding of this relationship between magnetic, electric, and optical factors of the spin-crossover transition is prerequisite for a thermodynamic basis for multiferroic behavior and magneto-electric coupling.

.

Supplementary Materials: Figure S1 contains X-ray absorption spectra taken at 250 K with and without the presence of an applied 1.8 T magnetic field. Reference X-ray absorption spectra of the [Fe{$H_2B(pz)_2$}$_2$(bipy)] low spin and high spin states are shown in Figure S2. The evolution of the high spin state at 250 K, with and without the presence of an applied 1.8 T magnetic field, is shown in Figure S3.

Preprints (www.preprints.org) | NOT PEER-REVIEWED | Posted: 18 August 2021 doi:10.20944/preprints202108.0377.v1

Author Contributions: For research articles with several authors, a short paragraph specifying their individual contributions must be provided. The following statements should be used "Conceptualization, A.T.N., P.A.D. and R.C; methodology, A.T.N., J.F., P.A.D. and R.C; software, A.T.N., J.F.; validation, G.H., A.T.N., A.S.D., P.A.D.. and R.C.; formal analysis, G.H., T.K.E., A.S.D, A.T.N., S.Y., P.A.D.; investigation, G.H., A.T.N., T.K.E., A.S.D., X.J., E.M., C.M., S.Y., J.Z., R.C., and X.X.; resources, X.J., C.M., S.Y., J.Z., R.C., and X.X.; data curation, G.H., A.S.D., and T.K.E.; writing—original draft preparation, G.H., A.T.N., and P.A.D.; writing—review and editing, A.T.N. and P.A.D; supervision, A.T.N. P.A.D., and R.C.; project administration, A.T.N. P.A.D., and R.C.; funding acquisition, A.T.N P.A.D., and R.C. All authors have read and agreed to the published version of the manuscript..

Funding: This research was supported by the National Science Foundation through NSF-DMR 2003057 [G. Hao, T. Ekanayaka, P. A. Dowben] and the EPSCoR RII Track-1: Emergent Quantum Materials and Technologies (EQUATE), Award OIA-2044049 [X. Jiang, C. Mellinger, X. Xu,]. Use of the Advanced Light Source, Lawrence Berkeley National Laboratory, was supported by the U.S. Department of Energy (DOE) under contract no. DE-AC02-05CH11231, while use of the Advanced Photon Source was supported by DOE's Office of Science under contract DE-AC02-06CH11357. G. Hao was partly supported by and Advanced Light Source Graduate student fellowship throughout this effort.

Data Availability Statement: The data presented in this study arises from the sources cited or are available on request from the corresponding authors.

Conflicts of Interest: The authors declare no conflict of interest. The funders had no role in the design of the study; in the collection, analyses, or interpretation of data; in the writing of the manuscript, or in the decision to publish the results.

Appendix A

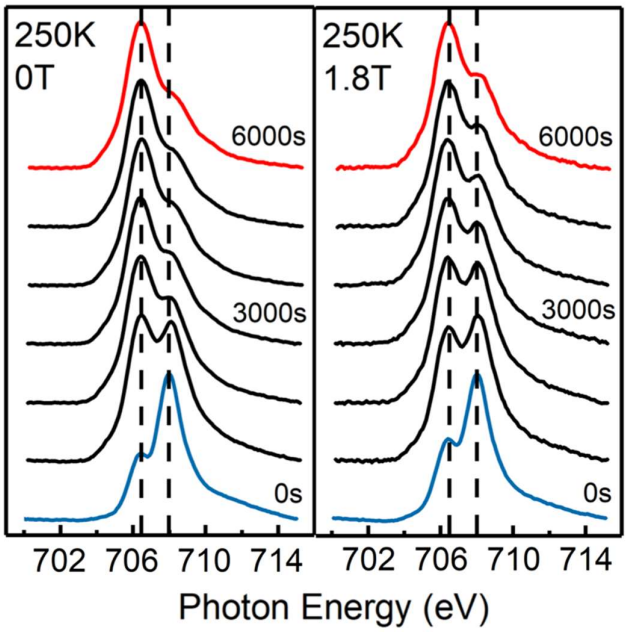

Figure S1. The time evolution of the X-ray absorption spectra with and without an applied 1.8T magnetic field of $[Fe\{H_2B(pz)_2\}_2(bipy)]$, under a constant incident X-ray fluence at 250 K. The spectra in blue are indicative of the low spin state, while the spectra in red are largely indicative of the high spin state.

Preprints (www.preprints.org) | NOT PEER-REVIEWED | Posted: 18 August 2021 doi:10.20944/preprints202108.0377.v1

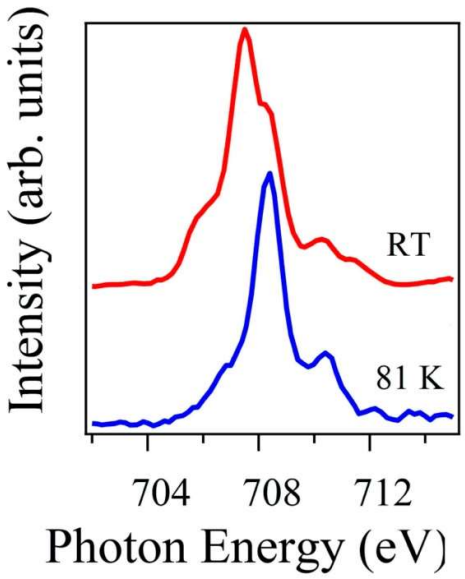

Figure S2. Higher resolution X-ray absorption spectra showing an example of reference spectra for the high spin state and low spin state of [Fe{H$_2$B(pz)$_2$}$_2$(bipy)] above and below the accepted spin transition temperature in the region of 160 K. The reference spectra provide a facile mechanism for ascertaining spin state occupancy.

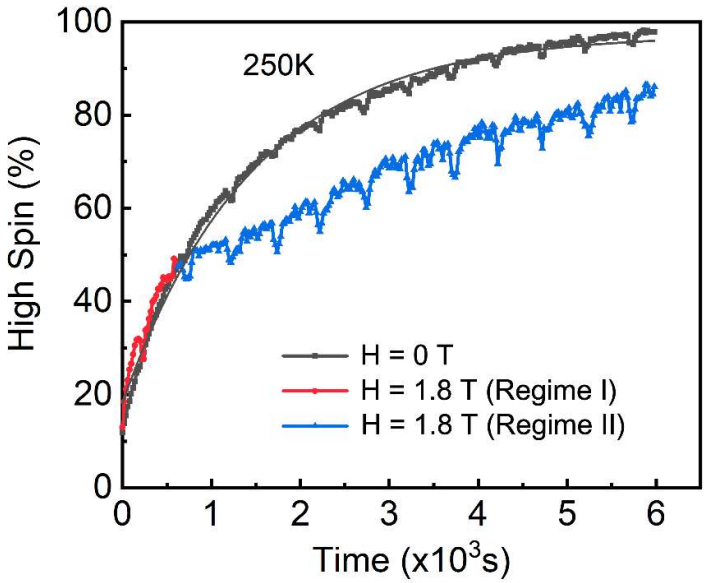

Figure S3. The evolution of the high spin state occupancy in the [Fe{H$_2$B(pz)$_2$}$_2$(bipy)] molecular thin film that accompany an incident soft X-ray fluence at 250 K, in the absence of an applied magnetic field (black) as well as in the presence of a 1.8 T applied magnetic field (red and blue). Exponential fit to the high spin state conversion in the field-free case is indicated as a thin solid black line.

References

1. Fiebig, M. Revival of the magnetoelectric effect. *J. Phys. D. Appl. Phys.* 2005, **38,** R123–52
2. Curie, P. Sur la symétrie dans les phénomènes physiques, symétrie d'un champ électrique et d'un champ magnétique. *J. Phys. Théorique Appliquée* 1894, **3,** 393–415

Preprints (www.preprints.org) | NOT PEER-REVIEWED | Posted: 18 August 2021 doi:10.20944/preprints202108.0377.v1

3. Sharma, N.; Bird, J. P.; Binek, C.; Dowben, P. A.; Nikonov, D.; Marshall, A. Evolving magneto-electric device technologies. *Semicond. Sci. Technol.* 2020, **35,** 073001
4. International Roadmap for Devices and Systems 2020 *IEEE* https://irds.ieee.org/editions/2020
5. Chikara, S.; Gu, J.; Zhang, X. G.; Cheng, H. P.; Smythe, N.; Singleton, J.; Scott, B.; Krenkel, E.; Eckert, J.; Zapf, V. S. Magnetoelectric behavior via a spin state transition. *Nat. Commun.* 2019, **10,** 1–8
6. Otsuki ,Y.; Kimura, S.; Awaji, S.; Nakano, M. Magnetocapacitance effect and magnetostriction by the field-induced spin-crossover in [MnIII(taa)]. *AIP Adv.* 2019, **9,** 8
7. Jakobsen, V. B.; Chikara, S.; Yu, J.-X.; Dobbelaar, E.; Kelly, C. T.; Ding, X.; Weickert, F.; Trzop, E.; Collet, E.; Cheng, H.-P.; Morgan, G. G.; Zapf, V. S. Giant Magnetoelectric Coupling and Magnetic-Field-Induced Permanent Switching in a Spin Crossover Mn(III) Complex. *Inorg. Chem.* 2021, **60**, 6167-6175
8. Yum J.-X.; Chen, D.-T.; Gu, J.; Chen, J.; Jiang, J.; Zhang, L.; Yu, Y.; Zhang, X.-G.; Zapf, V. S.; Cheng, H.-P. Three Jahn-Teller States of Matter in Spin-Crossover System Mn(taa) *Phys. Rev. Lett.* 2020, **124,** 227201
9. Zapf, V. S.; Sengupta, P.; Batista, C. D.; Nasreen, F.; Wolff-Fabris, F.; Paduan-Filho, A. Magnetoelectric effects in an organometallic quantum magnet. *Phys. Rev. B* 2011, **83,** 140405
10. Kimura, S.; Narumi, Y.; Kindo, K.; Nakano, M.; Matsubayashi, G. Field-induced spin-crossover transition of Mn(taa) studied under pulsed magnetic fields. *Phys. Rev. B* 2005, **72,** 064448
11. Bousseksou, A.; Negre, N.; Goiran, M.; Salmon, L.; Tuchagues, J.-P.; Boillot, M.-L.; Boukheddaden, K.; Varret, F. Dynamic triggering of a spin-transition by a pulsed magnetic field *Eur. Phys. J. B* 2000, **13,** 451–6
12. Zhang, X.; N'Diaye, A. T.; Jiang, X.; Zhang, X.; Yin, Y.; Chen, X.; Hong, X.; Xu, X.; Dowben, P. A. Indications of magnetic coupling effects in spin cross-over molecular thin films. *Chem. Commun.* 2018, **54,** 944–7
13. Ketsle, G. A.; Levshin, L. V.; Mel'nikov, G. V.; Minaev, B. F. Effect of a magnetic field on delayed fluorescence of anthracene exciplexes *J. Appl. Spectrosc.* 1981, **34,** 287–91
14. Hodges, M. P. P.; Grell, M.; Morley, N. A.; Allwood, D. A. Wide Field Magnetic Luminescence Imaging. *Adv. Funct. Mater.* 2017, **27,** 1606613
15. Klein, G.; Voltz, R.; Schott, M.; Magnetic field effect on prompt fluorescence in anthracene: evidence for singlet exciton fission *Chem. Phys. Lett.* 1972, **16,** 340–4
16. Kalinowski, J.; Godlewski, J. Magnetic field effects on recombination radiation in tetracene crystal. *Chem. Phys. Lett.* 1975, **36,** 345–8
17. Ern, V.; Merrifield, R. E. Magnetic Field Effect on Triplet Exciton Quenching in Organic Crystals *Phys. Rev. Lett.* 1968, **21,** 609–11
18. Piland, G. B.; Burdett, J. J.; Kurunthu, D.; Bardeen, C. J.; Magnetic Field Effects on Singlet Fission and Fluorescence Decay Dynamics in Amorphous Rubrene *J. Phys. Chem. C* 2013, **117,** 1224–36
19. Zhang, X.; Costa, P. S.; Hooper, J.; Miller, D. P.; N'Diaye, A. T.;, Beniwal, S.; Jiang, X.; Yin, Y.; Rosa, P.; Routaboul, L.; Gonidec, M.; Poggini, L.; Braunstein, P.; Doudin, B.; Xu, X.; Enders, A.; Zurek, E.; Dowben, P. A. Locking and Unlocking the Molecular Spin Crossover Transition *Adv. Mater.* 2017, **29,** 1702257
20. Zhang, X.; Mu, S.; Chastanet, G.; Daro, N.; Palamarciuc, T.; Rosa, P.; Létard, J.-F.; Liu, J.; Sterbinsky, G. E.; Arena, D. A.; Etrillard, C.; Kundys, B.; Doudin, B.; Dowben, P. A. Complexities in the Molecular Spin Crossover Transition *J. Phys. Chem. C* 2015, **119,** 16293–302
21. Jiang, X.; Hao, G.; Wang, X.; Mosey, A.; Zhang, X.; Yu, L.; Yost, A. J.; Zhang, X.; DiChiara, A. D.; N'Diaye, A. T.; Cheng, X.; Zhang, J.; Cheng, R.; Xu, X.; Dowben, P. A. Tunable spin-state bistability in a spin crossover molecular complex *J. Phys. Condens. Matter* 2019, **31,** 315401
22. Warner, B.; Oberg, J. C.; Gill, T. G.; El Hallak F.; Hirjibehedin, C. F.; Serri, M,; Heutz, S.; Arrio, M.-A.; Sainctavit, P.; Mannini, M.; Poneti, G.; Sessoli, R.; Rosa, P. Temperature- and Light-Induced Spin Crossover Observed by X-ray Spectroscopy on Isolated Fe(II) Complexes on Gold. *J. Phys. Chem. Lett.* 2013, **4,** 1546–52
23. Mosey, A.; Dale, A. S.;, Hao, G.; N'Diaye, A.; Dowben, P. A.; Cheng, R. Quantitative Study of the Energy Changes in Voltage-Controlled Spin Crossover Molecular Thin Films. *J. Phys. Chem. Lett.* 2020, **11,** 8231–7
24. Hao, G.; Mosey, A.; Jiang, X.; Yost, A. J.; Sapkota, K. R.; Wang, G. T.; Zhang, X.; Zhang, J.; N'Diaye, A. T.; Cheng, R.; Xu, X.; Dowben, P. A. Nonvolatile voltage controlled molecular spin state switching. *Appl. Phys. Lett.* 2019, **114,** 032901
25. Kipgen, L.; Bernien, M.; Nickel, F.; Naggert, H.; Britton, A. J.; Arruda, L. M.; Schierle, E.; Weschke, E.; Tuczek, F.; Kuch, W. Soft-x-ray-induced spin-state switching of an adsorbed Fe(II) spin-crossover complex. *J. Phys.: Condens. Matter* 2017, **29,** 394003
26. Kipgen, L.; Bernien, M.; Ossinger, S.; Nickel, F.; Britton, A. J.; Arruda, L. M.; Naggert, H.; Luo, C.; Lotze, Ch.; Ryll, H.; Radu, F.; Schierle, E.; Weschke, E.; Tuczek, F.; Kuch, W. Evolution of cooperativity in the spin transition of an iron(II) complex on a graphite surface. *Nat. Commun.* 2018, **9,** 2984
27. Costa, P.; Hao, G.; N'Diaye, A. T.; Routaboul, L.; Braunstein, P.; Zhang, X.; Zhang, J.; Doudin, B.; Enders, A.; Dowben, P. A. Perturbing the spin crossover transition activation energies in Fe($H_2B(pz)_2)_2$(bipy) with zwitterionic additions. *J. Phys. Condens. Matter* 2018, **30,** 305503
28. Palamarciuc, T.; Oberg, J. C.; El Hallak, F.; Hirjibehedin, C. F.; Serri, M.; Heutz, S.; Létard, J.-F.; Rosa, P. Spin crossover materials evaporated under clean high vacuum and ultra-high vacuum conditions: from thin films to single molecules *J. Mater. Chem.* 2012, **22** 9690

Preprints (www.preprints.org) | NOT PEER-REVIEWED | Posted: 18 August 2021 doi:10.20944/preprints202108.0377.v1

29. Moliner, N.; Salmon, L.; Capes, L.; Muñoz, M. C.; Létard, J.-F.; Bousseksou, A.; Tuchagues, J.-P.; McGarvey, J. J.; Dennis, A. C.; Castro, M.; Burriel, R.; Real, J. A. Thermal and Optical Switching of Molecular Spin States in the {[FeL[$H_2B(pz)_2]_2$} Spin-Crossover System (L = bpy, phen). *J. Phys. Chem. B* 2002, **106** 4276–83
30. Real, J. A.; Muñoz, M. C.; Faus, J.; Solans, X. Spin Crossover in Novel Dihydrobis(1-pyrazolyl)borate [$H_2B(pz)_2$]-Containing Iron(II) Complexes. Synthesis, X-ray Structure, and Magnetic Properties of [FeL{$H_2B(pz)_2$}$_2$] (L = 1,10-Phenanthroline and 2,2'-Bipyridine). *Inorg. Chem.* 1997, **36,** 3008–13
31. Chen, C. T.; Idzerda, Y, U.; Lin, H.-J.; Smith, N. V.; Meigs, G.; Chaban, E.; Ho, G. H.; Pellegrin, E.; Sette, F. Experimental confirmation of the X-ray magnetic circular dichroism sum rules for iron and cobalt. *Phys. Rev. Lett.* 1995, **75**, 152
32. Zhang, X.; Palamarciuc, T.; Létard, J.-F.; Rosa, P.; Lozada, E. V.; Torres, F.; Rosa, L. G.; Doudin, B.; Dowben, P. A.; The spin state of a molecular adsorbate driven by the ferroelectric substrate polarization *Chem. Commun.* 2014, **50,** 2255
33. Weber, B. "Koordinationschemie Grundlagen und aktuelle Trends", Springer Spectrum, Springer Verlag (Berlin, Heidelberg), 2014; doi: 10.1007/978-3-642-416850-9
34. Hao, G.; Cheng, R.; Dowben, P. A. The emergence of the local moment molecular spin transistor *J. Phys. Condens. Matter* 2020, **32,** 234002
35. Zhen, C.; Zhang, X.; Wei, W.; Guo, W.; Pant, A.; Xu, X.; Shen, J.; Ma, L.; Hou, D. Nanostructural origin of semiconductivity and large magnetoresistance in epitaxial $NiCo_2O_4/Al_2O_3$ thin films. *J. Phys. D. Appl. Phys.* 2018, **51,** 145308
36. Mellinger, C.; Waybright, J.; Zhang, X.; Schmidt, C.; Xu, X. Perpendicular magnetic anisotropy in conducting $NiCo_2O_4$ films from spin-lattice coupling. *Phys. Rev. B* 2020, **101,** 014413
37. https://www.aps.anl.gov/Sector-4/4-ID-C/Instrumentation
38. Shepit, M.; Paidi, V. K.; Roberts, C. A.; Reddy, G. K.; van Lierop, J. Unusual magnetism in $Cu_xCo_{3-x}O_4$ nanoparticles *Physical Review B* 2021, **103**, 024448